Antiferromagnetic-ferromagnetic crossover in $La_{0.5}Pr_{0.5}Mn_2Si_2$ and its consequences on magnetoelastic and magnetocaloric properties

B. Emre,[1] S. Aksoy,[2] O. Posth,[2] M. Acet,[2] E. Duman,[3] J. Lindner,[2] and Y. Elerman[1]
[1]*Department of Engineering Physics, Ankara University, 06100 Besevler-Ankara, Turkey*
[2]*Experimentalphysik, Universität Duisburg, Essen, D-47048 Duisburg, Germany*
[3]*Institut für Physik der kondensierten Materie, Heinrich Heine Universität, D-40225 Düsseldorf, Germany*
(Received 12 May 2008; published 9 October 2008)

$La_{0.5}Pr_{0.5}Mn_2Si_2$ exhibits an antiferromagnetic-ferromagnetic transition caused by the crossover of the critical distance between Mn atoms on changing temperature. Applying a magnetic field in the antiferromagnetic state can cause a field-induced transformation to the ferromagnetic state at a critical field, which increases with decreasing temperature. We study here with magnetization and strain measurements the magnetic-field-induced strain associated with the field-induced transformation and magnetocaloric effects close to the transition temperature. We also examine the temperature dependence of the critical field and find from magnetization and ferromagnetic resonance measurements that short-range ferromagnetic correlation among the rare earth and Mn-sublattices occur at low temperatures. At low temperatures, this causes a decrease in the critical field for the crossover from antiferromagnetic to ferromagnetic coupling with decreasing temperature.

DOI: 10.1103/PhysRevB.78.144408 PACS number(s): 75.30.Cr, 75.50.−y

I. INTRODUCTION

Rapid changes in the magnetization M with respect to temperature T is a favorable property for the occurrence of large magnetocaloric effects (MCE) since the size of an entropy change ΔS is governed by the size of dM/dT (other than the size of M itself) in the relationship $\Delta S = \int (dM/dT)dH$, where H is the magnetic field. A rapid change is found at the paramagnetic (PM)/ferromagnetic transition in Gd metal, which has proved to be a useful magnetocaloric material showing a reversible MCE.[1] Rapid changes also occur in the temperature vicinity of structural phase transitions because the magnetic exchange and along with it the nature of magnetic coupling in each of the structures above and below the transition temperature can be different. Such effects are found in a variety of systems, such as Gd-Si-Ge-based alloys exhibiting the giant MCE and the Heusler-based alloys exhibiting the inverse MCE.[1–3] However, the structural transition occurring in these systems imposes a limitation on the reversibility of the MCE because of the presence of a thermal hysteresis associated with the transition.

Another category of materials that exhibit substantial inverse MCE are those that undergo antiferromagnetic (AF)-ferromagnetic (FM) transitions and are found in a variety of intermetallic alloys and compounds.[4–6] In many cases, these transitions are free of thermal hysteresis—a property which makes such systems particularly attractive as magnetic refrigerants.

In systems undergoing AF/FM transitions, considerable changes in the lattice dimensions can also occur at the transition. If the transition is hysteresis free and can be driven by an isothermally applied magnetic field close to the transition temperature, large reversible magnetic-field-induced strains (MFIS) can be expected to occur. Such effects referred to as magnetic superelasticity is found in some Heusler-based alloys that undergo martensitic transformations.[7,8] Here again, the presence of a structural transformation imposes limitations on the reversibility of the strain on removing the magnetic field.

Studies have shown that there are a number of rare-earth manganese silicides and germanides that undergo AF/FM transitions. This transition takes place at a temperature where the Mn-Mn atomic separation crosses a critical value of 0.287 nm, and some of these occur in a narrow temperature range.[5,9] These materials are magnetically anisotropic and considerable differences in the lattice parameters between the AF and FM states are observed. In $La_{0.5}Pr_{0.5}Mn_2Si_2$, the temperature width of the AF/FM transition is around 30–50 K being relatively narrow with respect to other rare-earth-based manganese silicides and germanides. This material is body-centered-tetragonal, and the relative changes in the a and c lattice parameters $\Delta a/a$ and $\Delta c/c$ are 0.15% and −0.08%, respectively.[10] The associated change in the unit-cell volume $\Delta V/V$ is 0.22%. The occurrence of a magnetic-field-induced AF/FM transition in this material, along with large dimensional changes, makes it an interesting candidate as a large MFIS material with reversible strain. In the following, we first investigate the magnetic properties related to the field-induced AF/FM transition by magnetization and ferromagnetic resonance (FMR) studies of $La_{0.5}Pr_{0.5}Mn_2Si_2$. We then present results on the magnetoelastic properties and the entropy change in the vicinity of the transition.

II. EXPERIMENT

$La_{0.5}Pr_{0.5}Mn_2Si_2$ was prepared by arc melting La, Pr, Mn, and Si constituents under argon atmosphere. The structure of the samples was checked by x-ray diffraction using Cu-$K\alpha$ radiation.

Magnetization measurements as a function of temperature $M(T)$ and magnetic field $M(H)$ were carried out in the temperature range $5 \leq T \leq 350$ K and up to 5 T with a superconducting quantum interference device magnetometer. For the $M(T)$ measurements, the samples were first taken to a temperature above 350 K and measured on cooling to low tem-

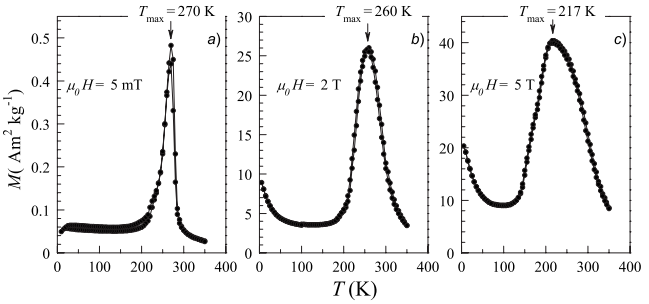

FIG. 1. Temperature dependence of the magnetization in (a) 5 mT, (b) 2 T, and (c) 5 T. T_{max} denotes the temperature corresponding to the maximum in $M(T)$

peratures (field cooled, FC) and, subsequently, on heating back up to 350 K (field heated, FH).

FMR experiments were carried out at a microwave frequency of 9.29 GHz in the temperature interval $5 \leq T \leq 330$ K on a powder sample. The external magnetic field was swept up to 1.4 T, and resonance spectra were recorded as a function of temperature. The external magnetic field was modulated at a frequency of 100 kHz using modulation amplitudes of up to 3 mT. The signal was detected using lock-in technique, thus the derivative of the absorption signal was recorded (for details on FMR, see Refs. 11–13).

Strain measurements as a function of temperature $(\Delta l/l)(T)$ in constant fields and as a function of field $(\Delta l/l)(H)$ at constant temperature were carried out using strain gages.

III. RESULTS

A. Temperature dependence of the magnetization

$M(T)$ in applied fields of 50 mT, 2 T, and 5 T is shown in Fig. 1. The features in $M(T)$ are similar for the FC and FH measurements for all applied fields. A structural transformation accompanying the AF/FM transition is apparently absent since this would have led to a hysteresis around the transition. Only a small difference between the FC and FH states, between 50 K and about 200 K, is observed in the 5 mT measurement shown in Fig. 1(a). At low temperatures, $M(T)$ exhibits a small feature around 30 K in Fig. 1(a). This feature enhances as the applied field increases as seen in Fig. 1(b) and is observed as a decrease in $M(T)$ with increasing temperature. It becomes stronger in Fig. 1(c). For temperatures up to about 200 K in Fig. 1(a), the interlayer magnetic coupling of the Mn sublattice is AF with a canting angle of about 34° with the c axis.[10] On further increasing the temperature, FM coupling along the c axis of the Mn sublattice sets in and $M(T)$ runs through a maximum at T_{max}, above which $M(T)$ begins to decrease as the FM state destabilizes. At higher temperatures, there is only intralayer AF ordering in the Mn sublattice up to $T_N^{intra} \approx 400$ K.[5] T_{max} decreases with increasing applied measuring field as seen in Figs. 1(b) and 1(c). The values of T_{max} are 270, 260, and 217 K for 50 mT, 2 T, and 5 T, respectively, corresponding to a rate of change in T_{max} with respect to field of about 10 K T^{-1}.

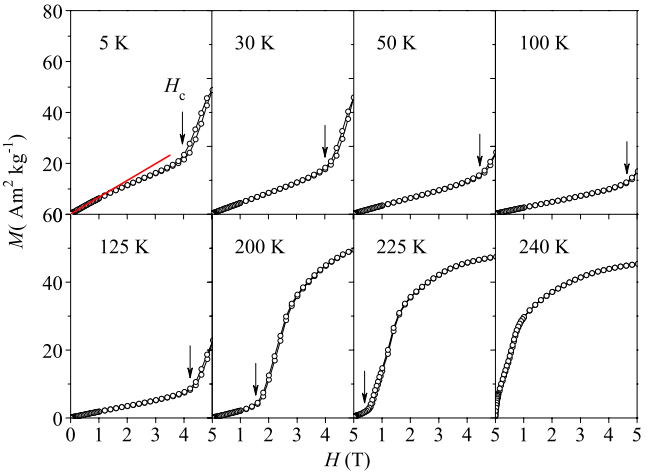

FIG. 2. (Color online) Magnetic-field dependence of the magnetization for $0 \leq \mu_0 H \leq 5$ T in the temperature interval $10 \leq T \leq 240$ K. H_c corresponds to the field at the onset of the AF/FM transition. The line is fitted to the low-field data at 5 K shows the nonlinear nature of $M(H)$ at this temperature.

B. Field-induced AF/FM transition

Figure 2 shows the magnetic-field dependence of the magnetization $M(H)$ for $0 \leq \mu_0 H \leq 5$ T at some selected temperatures in the interval $5 \leq T \leq 240$ K. The data are taken on increasing and decreasing field, and no magnetic hysteresis is observed. The curves show the onset of crossover from the AF to the FM state at the critical field H_c indicated by arrows. For fields $H \leq H_c$, the magnetization increases linearly with increasing field as expected for an antiferromagnet except for some nonlinearities at low fields in the data taken at 5 K that are expected to be related to the presence of short-range FM correlations developing through the interaction between the Mn and the rare-earth sublattices. The line fitted through the low-field data at 5 K makes this deviation clear. Above H_c, the increase is initially faster and tends to saturation at higher fields, as can be seen in the data taken at 200 and 225 K. The value of H_c first increases with increasing temperature at low temperatures and then eventually begins to decrease as the AF/FM transition is approached.

The temperature dependence of the magnetic susceptibility $\chi(T)$ is also plotted in Fig. 3 in the AF temperature range at a field of 500 Oe. This field is selected since it lies in a range where $M(H)$ shows linearity up to the stability limit of the AF phase. $\chi(T)$ shows a decrease with increasing temperature which is opposite to what is expected from a conventional antiferromagnet. $\chi(T)$ begins to increase with increasing temperature only roughly above 180 K.

The temperature dependence of H_c is plotted in Fig. 4. On increasing temperature, H_c reaches a distinct maximum at about 90 K after which it decreases to zero at about 240 K. The reason why H_c runs through a maximum is closely related to the presence of ferromagnetic correlations at low temperatures which gives rise to the features in $M(T)$ and $M(H)$ shown above (cf. Fig. 1). This will be further discussed in Sec. IV.

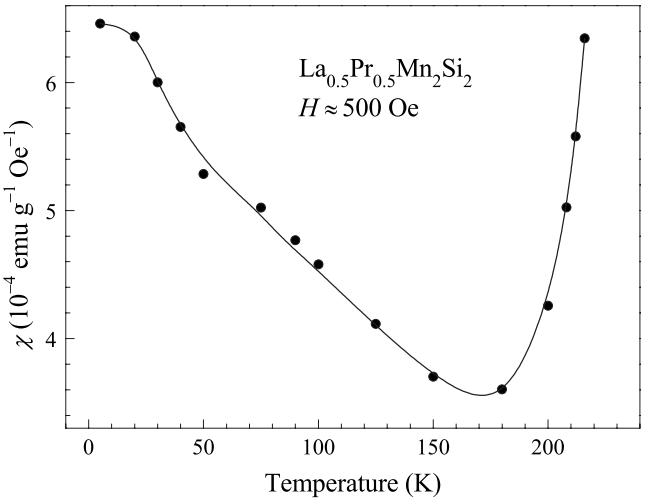

FIG. 3. $\chi(T)$ in the AF state of $La_{0.5}Pr_{0.5}Mn_2Si_2$ at 500 Oe.

C. Ferromagnetic resonance

To obtain more detailed information on the magnetic properties and to give further details related to the field-induced AF/FM transition, we have undertaken FMR studies. Figure 5 shows two selected FMR spectra at 300 and 20 K recorded in the field range $0 \leq \mu_0 H \leq 1.2$ T. The spectrum taken at 300 K shows one signal in the complete field range. This signal, labeled as I, is observed in all spectra in the interval $5 \leq T \leq 330$ K. Below temperatures of about 50 K, a second signal, labeled as II, emerges at field values lower than that corresponding to signal I. At 20 K, the signal is observed at about 550 mT as seen in the figure.

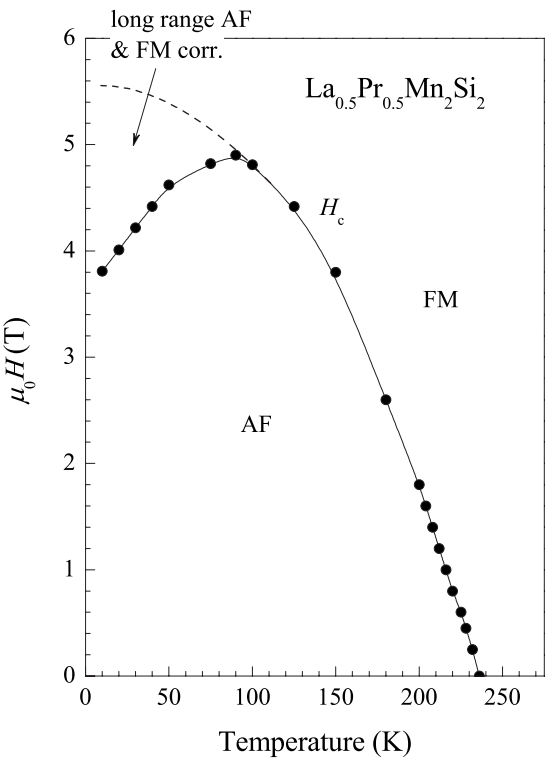

FIG. 4. $\mu_0 H$ as a function of temperature. H_c determined from the measurements has a maximum at about 90 K. The decrease in H_c below 90 K is attributed to the development of FM correlations among the rare-earth and Mn-sublattices (see Sec. IV).

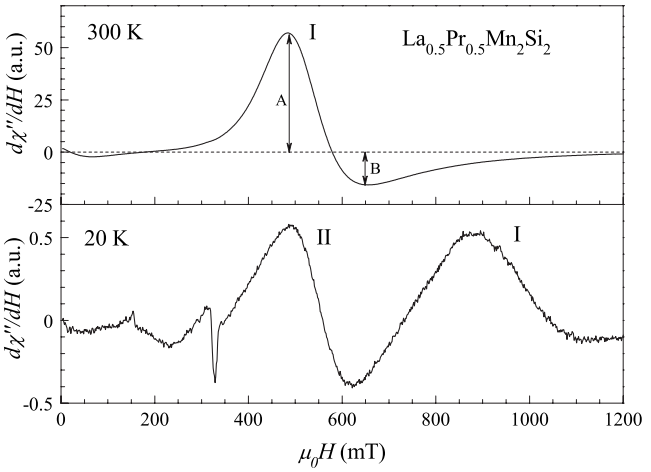

FIG. 5. FMR measurement for $T=300$ and 20 K. The signal at 300 K is attributed to an antiferromagnetic phase. At $T=20$ K aside from the antiferromagnetic contribution (I) which is shifted toward higher magnetic-field values, an additional signal is observed which is assigned to a second ferromagnetic (II) magnetic phase within the sample. The small signal at 320 mT results from a paramagnetic (PM) contribution. A and B in the upper panel are the heights referred to in the Sec. IV.

The temperature dependence of the resonance fields H^I_{res} and H^{II}_{res} extracted from the two signals according Dyson's treatment of bulk specimens[14] are shown in Fig. 6. Below 330 K, H^I_{res} increases and reaches a maximum at about 295 K. This behavior is related to weak antiferromagnetic ordering, as will be discussed in Sec. III C 1 and is consistent with the observed intralayer AF-ordering in the Mn-sublattice below the Néel temperature of about 400 K.[5] When the temperature is further decreased, the resonance field falls below the isotropic value $\omega/\gamma \approx 330$ mT, where ω is the micro-

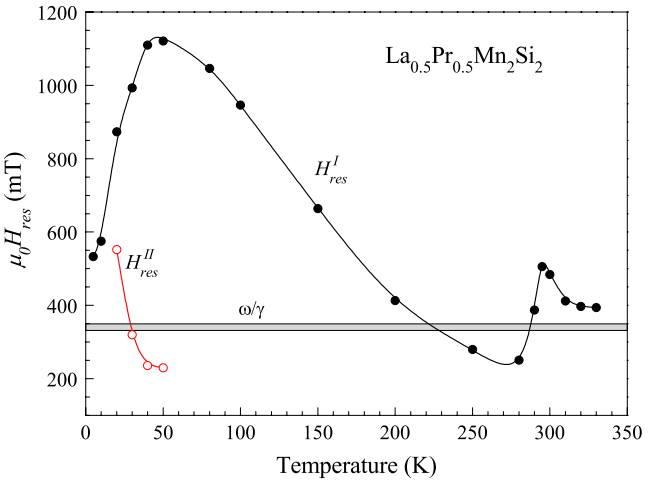

FIG. 6. (Color online) Temperature dependence of the resonance field for the antiferromagnetic phase (I) and the ferromagnetic correlations which appear at low temperatures (II). The heavy line indicates the isotropic value ω/γ.

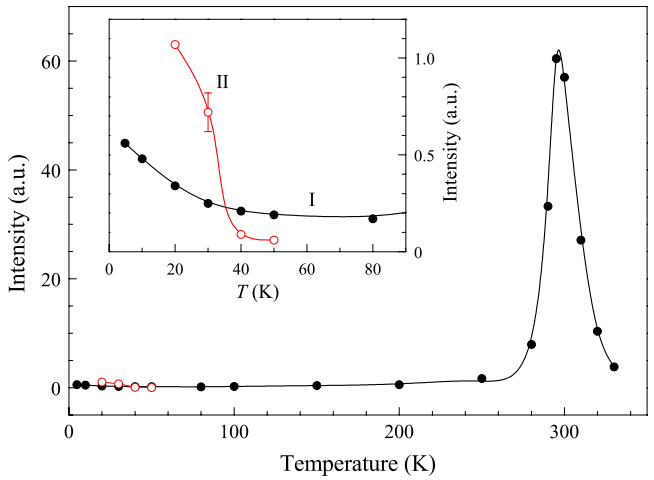

FIG. 7. (Color online) Temperature dependence of the intensity for the antiferromagnetic (squares) and the ferromagnetic phases (triangles). The inset shows the low-temperature data in detail. The error bar is typical for all data.

wave frequency and γ is the gyromagnetic ratio given as $g\mu_B/H$ with g being the g factor (taken here as 2) and μ_B as the Bohr magneton. This value is indicated in the figure with the heavy line. By the arguments given in Sec. IV [Eq. (1)], this indicates that the Mn sublattice mainly orders ferromagnetically in the range $230 \leq T \leq 290$ K being consistent with the observed interlayer ferromagnetic ordering in the Mn-sublattice.[5] Using the same argument used for explaining the data at $T > 330$ K, one can conclude that antiferromagnetism reappears below $T = 230$ K. This is consistent with the behavior of $M(T)$ (Fig. 1) and the occurrence of Mn-interlayer coupling observed in this system.[5]

H_{res}^{II} lies below the isotropic value, and, therefore, we assign it to the development of ferromagnetic correlations through the exchange interactions among the Pr species in the rare-earth sublattice and the moments in the Mn sublattice as also suggested by the $M(H)$ data at low temperatures. As the temperature decreases, the antiferromagnetic and the ferromagnetic phases couple. Therefore, H_{res}^{II} increases with decreasing temperature while H_{res}^{I} of the AF phase of Mn sublattice decreases. As the values of both resonance fields approach each other at low temperatures, the coupling of both phases become strongest, and effectively only one signal is observed. This scenario thus confirms the results given above, namely, that at low temperatures, long-range AF order and local FM correlations are present.

The temperature dependence of the FMR intensity, which is a measure of the magnetic moment, is shown in Fig. 7. One sees here a similar behavior as for $M(T)$ in Fig. 1. In the intermediate temperature range $50 \leq T \leq 230$ K, where interlayer AF coupling is present, the intensity is small, but at temperatures lower than 50 K, where signal II emerges, it increases again. This is consistent with an appearance of ferromagnetic order that leads to an increase in the overall magnetic moment of the sample. One should note that also the intensity of signal I increases below 50 K. This again demonstrates the presence of an interaction between the antiferromagnetic and ferromagnetic regions within the sample, being in accordance with the low-temperature features in $M(T)$ shown in Fig. 1.

1. Absorption profiles and temperature dependence of the resonance fields

Before accounting for the behavior of the temperature dependence of the resonance fields and the intensities related to the two FMR signals, we discuss their absorption profiles. The spectral shape of signal I (Fig. 5) at $T = 300$ K agrees well with the so-called Dyson profile.[14,15] Such a profile results when electron diffusion through the sample become important. While a Lorentzian line shape is expected for the case in which the time it takes an electron to diffuse through the sample (t_{sample}) is much smaller than the time it takes the electron to diffuse through the skin depth (t_{skin}), the Dyson profile results for the opposite case ($t_{\mathrm{sample}} \gg t_{\mathrm{skin}}$). The first case is fulfilled for samples which are thinner than the microwave skin depth d_{skin}, whereas the latter is expected for samples thicker than d_{skin}. Our observation, therefore, leads to the conclusion that the particles in the powder sample must be larger than d_{skin}. According to Refs. 14 and 15 the ratio of the heights of the maximum and minimum in the derivative of the absorption curve A/B (see Fig. 5) is a measure of the ratio $R = t_{\mathrm{skin}}/t_1$, where t_1 is the relaxation time of the electron spin with respect to the microwave excitation. For $R \to \infty$ (slow-diffusion regime and low conductivity) a value of $A/B \to 2.7$ results. Note that $A/B = 2.7$ is also the expected value for completely stationary magnetic dipoles distributed within a thick specimen, each of them having a Lorentzian line shape.[14] For fast diffusing electrons or $R \to 0$ (high conductivity) $A/B \to 19$. At 300 K our experimental results for A/B is 3.6, showing that we are in the slow-diffusion regime. On lowering the temperature, the A/B-ratio becomes significantly larger, indicating that the diffusion time of the electrons in the sample decreases due to its higher conductivity.

In contrast to signal I, signal II emerging at lower temperatures $T < 50$ K has a more symmetric shape (smaller A/B ratio), implying a smaller R value. We note that the exact value for A/B cannot be extracted from the data due to the overlap of both resonances. The small R value could result from the fact that the contribution leading to signal II exhibits a smaller diffusion time due to higher resistivity. As the samples are, however, homogeneous and signal II appears only at low temperatures, we attribute its symmetrical shape to the fact that signal II results from local ferromagnetic correlations. The lateral dimensions of these correlations are assumed to be rather small so that each of them is expected to exhibit a Lorentzian line shape. The distribution of the local areas with FM correlations within the sample would then indeed lead to the observed symmetric line shape, in accordance with the expectation for the stationary limit ($R = 0$).[14,15]

To qualitatively understand the behavior of, in particular, signal I, one has to investigate the resonance equation that links the resonance frequency with the resonance field. For a ferromagnetically coupled lattice the equation reads[16]

$$B_{\mathrm{res}} = \frac{\omega}{\gamma} - B_A. \tag{1}$$

Here B_{res} is the resonance field and B_A is an internal anisotropy field. For simplicity the resonance equation is written under the assumption that the external magnetic field is aligned parallel to the internal anisotropy field. In a polycrystal, the anisotropy field orientation is randomly distributed over the sample volume so that the magnetization of the sample interacts with an effective anisotropy field. The resonance equation shows that the effect of the internal anisotropy field is to shift the resonance field toward smaller field values with respect to the isotropic resonance field ω/γ.

For an antiferromagnet, in which the magnetic sublattices are coupled by an exchange field B_E and for which B_A is additionally taken into account, the resonance equation for the case that the external magnetic field is oriented parallel to B_A is given by[17]

$$B_{\mathrm{res}} = \frac{\omega}{\gamma} \pm \sqrt{B_A(2B_E + B_A)}. \tag{2}$$

Here, two solutions are possible whereby the resonance field is shifted below or above ω/γ. For strong antiferromagnets B_E can have values of several tens of Tesla so that the solution shifted to fields lower than the isotropic value gives negative values. On the other hand, the solution shifted toward higher fields can only be observed for external magnetic-field values of the order of B_E. This leads to the fact that in strongly coupled antiferromagnets, either large external fields are needed (observation of the high-field solution) or the resonance, which would occur at microwave frequencies and negative resonance fields, has to be shifted to positive fields by using infrared light (antiferromagnetic resonance). For weakly coupled antiferromagnets, however, even at microwave frequencies, resonance may occur. Depending on the values of B_E and B_A, either one or even two signals can be expected for a given microwave frequency. Since in our case only one resonance is observed in the temperature regimes of AF coupling, we assume that the coupling strength (given by B_E) is sufficient to shift the low-field solution to below $B_{\mathrm{res}}=0$ so that only the high-field solution is excited in the experiment.

D. Temperature and magnetic-field dependence of strain

The temperature dependence of the strain $(\Delta l/l)(T)$ in constant magnetic fields of 0, 2, and 5 T is shown in Fig. 8. The arrows indicate the temperatures corresponding to the peak positions in $M(T)$. $(\Delta l/l)(T)$ increases with increasing temperature as the AF/FM transition is approached. Close to the transition, the increase becomes faster and eventually the increase resumes monotonously. The measurements are taken on increasing and decreasing temperature, and no thermal hysteresis is observed around the transitions at any applied measuring-field. The temperatures corresponding to T_{max} in Fig. 1 for 0, 2, and 5 T are shown with arrows. These temperatures lie nearly at the inflection point of the curves. As in the $M(T)$ data in Fig. 1, the transition temperatures here are also seen to decrease with increasing applied magnetic field. The difference in the relative length change between the FM and AF states $\Delta(l/l)_{\mathrm{AF/FM}}$ is observed to be approximately 0.1% at 5 T.

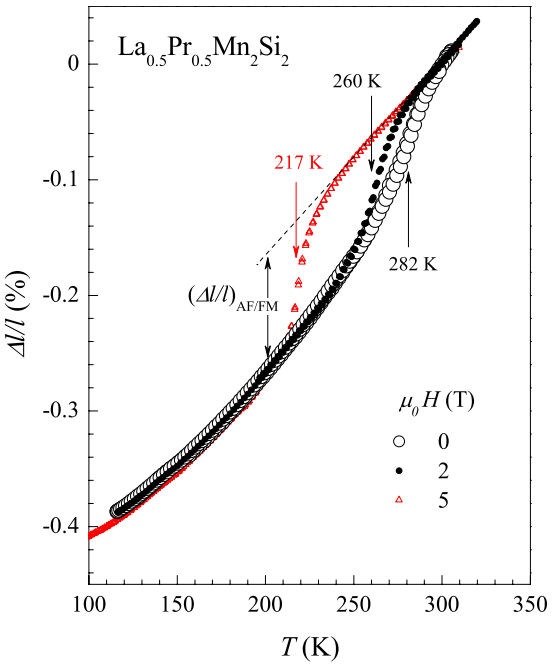

FIG. 8. (Color online) Temperature dependence of the strain in 0, 2, and 5 T. The arrows indicate to the temperatures corresponding to the peak positions in $M(T)$.

Figure 9 shows the magnetic-field dependence of strain at 252 and 272 K in the range $0 \leq \mu_0 H \leq 5$ T. 252 K was chosen as a measurement temperature to observe a maximum possible MFIS, and 272 K was chosen to find a MFIS of substantial magnitude; not necessarily maximum but occurring at a minimum possible magnetic field. The data show a MFIS of about 0.09% at 252 K, which is nearly the full strain of 0.1% obtained by measuring under constant magnetic field (Fig. 8). At 272 K a lower MFIS of about 0.06% is obtained; however a strain of about 0.03% is already attained at about 2 T in this polycrystalline material.

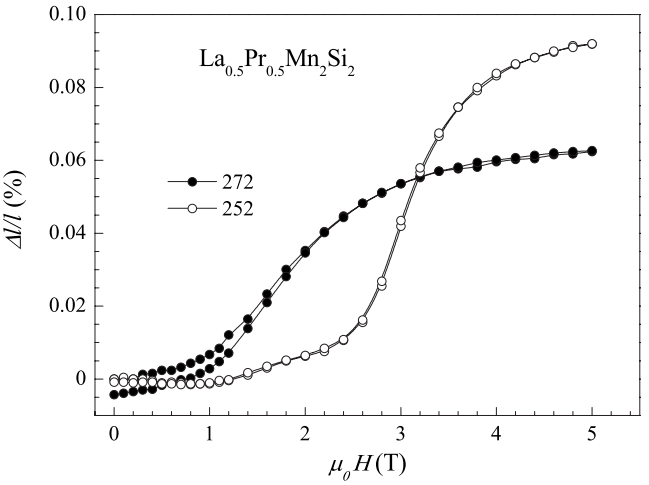

FIG. 9. Magnetic-field dependence of the strain for $0 \leq \mu_0 H \leq 5$ T at 252 and 272 K.

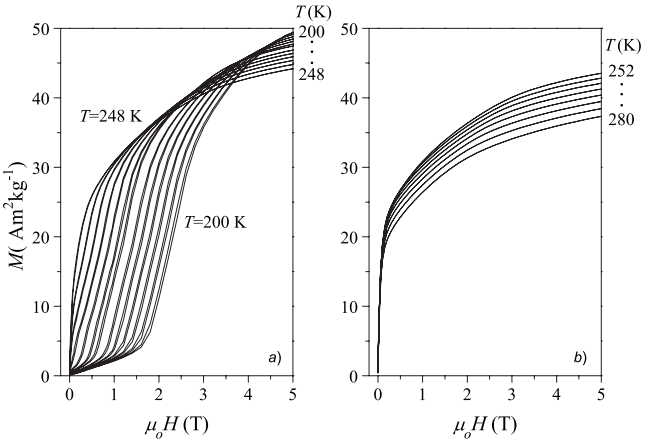

FIG. 10. $M(H)$ in the temperature interval (a) $200 \leq T \leq 248$ K and (b) $252 \leq T \leq 280$ K. The data are taken in steps of 4 K.

E. Magnetocaloric effects

$M(H)$ isotherms in the temperature range $200 \leq T \leq 280$ K are shown in Figs. 10(a) and 10(b). In Fig. 10(a), the results are shown for data taken in steps of 4 K on increasing and decreasing field in the temperature range $200 \leq T \leq 248$ K. Magnetic hysteresis is practically absent. The magnetic-field-induced AF/FM transition is observed above critical fields, as previously presented in Fig. 2. In Fig. 10(b), we show the data for $252 \leq T \leq 280$ K. In this set of data, no field-induced transition is observed.

The entropy change ΔS is calculated by numerically integrating the equation

$$\Delta S(T,H) = \mu_0 \int_0^H \left(\frac{\partial M}{\partial T}\right)_H dH. \tag{3}$$

As shown in Fig. 11, ΔS acquires positive and negative values corresponding, respectively, to the inverse and the conventional MCE. The crossover at about 250 K separates the temperature regions for which $dM/dT > 0$ and $dM/dT < 0$.

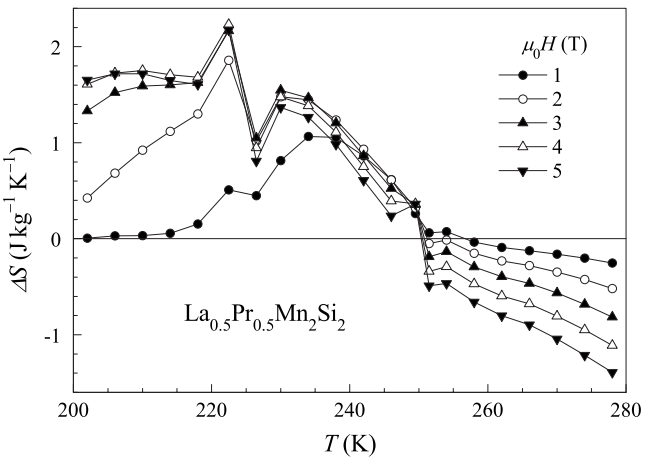

FIG. 11. Temperature dependence of the entropy change in $La_{0.5}Pr_{0.5}Mn_2Si_2$.

The inverse MCE at 5 T approaches values of roughly 2 J kg^{-1} K^{-1} around 220 K.

IV. DISCUSSION

$La_{0.5}Pr_{0.5}Mn_2Si_2$ undergoes both thermally and magnetically a hysteresis-free AF/FM transition. The hysteresis-free nature provides full reversibility for magnetic-field-induced strains and magnetocaloric effects. Especially in the case of MFIS, substantial reversible strains are attained already around 2 T, which is readily available in commercial permanent magnets. In single crystals, the maximum strain from geometrical considerations is expected to approach about 0.15%, which is comparable to the strain in Terfanol-D.[10] In $La_{0.5-x}Pr_xMn_2Si_2$ compounds, T_N^{inter} can be shifted from lowest temperatures to room temperature by adjusting x,[5] and, thereby, the position of the maximum in ΔS can be brought to the desired temperature. Although the MCE is not large compared to other giant MCE material in this particular compound, its hysteresis-free nature would be a source of motivation to study similar systems for large MCE.

Other than such technological implications, $La_{0.5}Pr_{0.5}Mn_2Si_2$ has low-temperature properties which are of physical interest. The parent compounds $LaMn_2Si_2$ and $PrMn_2Si_2$ show no long-range magnetic ordering in their rare-earth sublattices at low temperatures. However $PrMn_2Si_2$, which is AF in the Mn sublattice, shows strong nonlinearity in $M(H)$ at 5 K. This property is thought to be related to the interaction between Pr and Mn moments that onset at low temperatures and lead to short-range FM components configured among the rare earth (RE) and Mn sublattices. This property is evidently carried into $La_{0.5}Pr_{0.5}Mn_2Si_2$ as observed in the similar nonlinear behavior of $M(H)$ at low temperatures (Fig. 2) and has a strong influence on the field-induced transformation as evidenced by the anomalous temperature-behavior of χ and H_c (Figs. 3 and 4).

The decrease in H_c with increasing temperature on the high-temperature side of the maximum at about 90 K is caused by the weakening of AF exchange with respect to FM exchange as the AF/FM transition temperature above 200 K is approached. The decrease in χ with decreasing temperature is also a similar indication. For H_c to decrease with decreasing temperature below 90 K, the presence of a state at low temperatures having a magnetic configuration that weakens the AF exchange is required. The occurrence of short-range ferromagnetism at low temperatures is compatible with the nonlinearity in $M(H)$ at low temperatures (Fig. 2) and would weaken the AF exchange in the Mn sublattice, thereby accounting for the maximum in H_c. However, exactly how these correlations are configured among the rare earth and Mn sublattices cannot be extracted from the present data.

V. CONCLUSION

$La_{0.5}Pr_{0.5}Mn_2Si_2$ undergoes an AF to FM transition with increasing temperature. The FM state can also be reached by a field-induced transition from the AF to the FM state.

A consequence of the field-induced transformation is the large strain that are involved as well as substantial magnetocaloric effects. However, the critical-field associated with the transition shows anomalous temperature dependence, which can be accounted for by the occurrence of short-range ferromagnetic correlations occurring at low temperatures. We verify the presence of these correlations from the results of magnetization and ferromagnetic resonance experiments.

ACKNOWLEDGMENTS

This work was supported by BMBF(Germany)/TUBITAK(Turkey) under Project No. WTZ TUR04/11 and the Deutsche Forschungsgemeinschaft (SPP1239).

[1] V. K. Pecharsky and K. A. Gschneidner, Jr., Phys. Rev. Lett. **78**, 4494 (1997).
[2] O. Tegusa, E. Brück, L. Zhang, Dagula, K. H. J. Buschow, and F. R. de Boer, Physica B (Amsterdam) **319**, 174 (2002).
[3] T. Krenke, E. Duman, M. Acet, E. F. Wassermann, X. Moya, L. Mañosa, and A. Planes, Nature Mater. **4**, 450 (2005).
[4] S. A. Nikitin, G. Myalikgulyev, A. M. Tishin, M. P. Annaorazov, K. A. Asatryan, and A. L. Tyurin, Phys. Lett. A **148**, 363 (1990).
[5] E. Duman, M. Acet, I. Dincer, A. Elmali, and Y. Elerman, J. Magn. Magn. Mater. **309**, 40 (2007).
[6] K. G. Sandeman, R. Daou, S. Özcan, J. H. Durrell, N. D. Mathur, and D. J. Fray, Phys. Rev. B **74**, 224436 (2006).
[7] T. Krenke, E. Duman, M. Acet, E. F. Wassermann, X. Moya, L. Manosa, A. Planes, E. Suard, and B. Ouladdiaf, Phys. Rev. B **75**, 104414 (2007).
[8] R. Kainuma, Y. Imano, W. Ito, Y. Sutou, H. Morito, S. Okamoto, O. Kitakami, K. Oikawa, A. Fujita, T. Kanomata, and K. Ishida, Nature (London) **439**, 957 (2006).
[9] I. Dincer, Y. Elerman, A. Elmali, E. Ehrenberg, and G. André, J. Magn. Magn. Mater. **313**, 342 (2007).
[10] E. Duman, M. Acet, T. Krenke, E. Suard, and B. Ouladdiaf (unpublished).
[11] B. Heinrich and J. F. Cochran, Adv. Phys. **42**, 523 (1993).
[12] M. Farle, Rep. Prog. Phys. **61**, 755 (1998).
[13] J. Lindner and K. Baberschke, J. Phys.: Condens. Matter **15**, R193 (2003).
[14] G. Feher and A. F. Kip, Phys. Rev. **98**, 337 (1955).
[15] F. J. Dyson, Phys. Rev. **98**, 349 (1955).
[16] C. Kittel, Phys. Rev. **73**, 155 (1948).
[17] C. Kittel, Phys. Rev. **82**, 565 (1955).